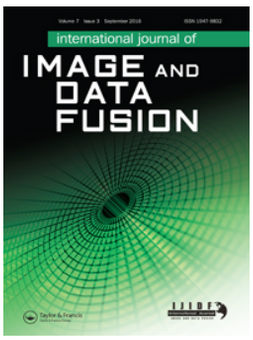

International Journal of Image and Data Fusion

ISSN: 1947-9832 (Print) 1947-9824 (Online) Journal homepage: http://www.tandfonline.com/loi/tidf20

Use of mobile LiDAR in road information inventory: a review

Haiyan Guan, Jonathan Li, Shuang Cao & Yongtao Yu

To cite this article: Haiyan Guan, Jonathan Li, Shuang Cao & Yongtao Yu (2016) Use of mobile LiDAR in road information inventory: a review, International Journal of Image and Data Fusion, 7:3, 219-242, DOI: 10.1080/19479832.2016.1188860

To link to this article: http://dx.doi.org/10.1080/19479832.2016.1188860

Published online: 17 Jun 2016.

Submit your article to this journal

Article views: 32

View related articles

View Crossmark data

Full Terms & Conditions of access and use can be found at
http://www.tandfonline.com/action/journalInformation?journalCode=tidf20

Download by: [University of Waterloo] **Date:** 13 September 2016, At: 07:15

INTERNATIONAL JOURNAL OF IMAGE AND DATA FUSION, 2016
VOL. 7, NO. 3, 219–242
http://dx.doi.org/10.1080/19479832.2016.1188860

Taylor & Francis
Taylor & Francis Group

REVIEW

Use of mobile LiDAR in road information inventory: a review

Haiyan Guan[a], Jonathan Li[b,c], Shuang Cao[a] and Yongtao Yu[d]

[a]College of Geography and Remote Sensing, Nanjing University of Information Science & Technology, Nanjing, China; [b]Key Laboratory of Sensing and Computing for Smart City, School of Information Science and Engineering, Xiamen University, Xiamen, China; [c]Department of Geography and Environment Management, University of Waterloo, Waterloo, Canada; [d]Faculty of Computer and Software Engineering, Huaiyin Institute of Technology, Huaian, China

ABSTRACT

Mobile LiDAR technology is currently one of the attractive topics in the fields of remote sensing and laser scanning. Mobile LiDAR enables a rapid collection of enormous volumes of highly dense, irregularly distributed, accurate geo-referenced data, in the form of three-dimensional (3D) point clouds. This technology has been gaining popularity in the recognition of roads and road-scene objects. A thorough review of available literature is conducted to inform the advancements in mobile LiDAR technologies and their applications in road information inventory. The literature review starts with a brief overview of mobile LiDAR technology, including system components, direct geo-referencing, data error analysis and geometrical accuracy validation. Then, this review presents a more in-depth description of current mobile LiDAR studies on road information inventory, including the detection and extraction of road surfaces, small structures on the road surfaces and pole-like objects. Finally, the challenges and future trends are discussed. Our review demonstrates the great potential of mobile LiDAR technology in road information inventory.

ARTICLE HISTORY
Received 10 January 2016
Accepted 8 May 2016

KEYWORDS
Mobile LiDAR; road information inventory; pavement cracks; roads; road markings; pole-like objects

1. Introduction

Remote-sensing technologies for road information inventory are undergoing rapid developments. The possibility of acquiring three-dimensional (3D) information of large-area roadways with survey-grade accuracy at traffic speeds is opening up new and efficient ways for road information inventory. Recent advances in sensor electronics and data treatment make these technologies affordable. The two major remote-sensing technologies that are popularly used in road information inventory are image-based and laser-based mobile mapping systems (Toth 2009). Mobile mapping systems collect street-level data more completely and efficiently than traditional surveying methods. Image-based mobile mapping systems have gained popularity in modelling and estimating road boundaries for road safety assistance (Dickmanns and Mysliwetz 1992, Pomerleau and Jochem 1996, Bertozzi *et al*. 1997) because the images contain rich information, such as colour and texture, beneficial for road extraction. Commercial

CONTACT Haiyan Guan guanhy.nj@nuist.edu.cn College of Geography and Remote Sensing, Nanjing University of Information Science & Technology, Nanjing, Jiangsu 210044, China

© 2016 Informa UK Limited, trading as Taylor & Francis Group

image-based road extraction systems have been widely available (Liu *et al*. 2013). However, image-based mobile mapping systems are limited to illumination and weather conditions, shadows cast by roadside buildings and trees, and occlusions caused by nearby moving vehicles and pedestrians (Tsogas *et al*. 2011). Moreover, the captured image data lack of accurate geospatial information and suffer greatly from distortions.

A laser-based mobile mapping system is flexibly mounted on any moving platforms, such as airplanes, cars/trucks, trains and boats. Future development continues to design a compact, lightweight and relatively inexpensive multipurpose mobile laser scanning system that should be quick and easy to deploy, and requires a minimum amount of existing equipment for operational support. An unmanned aerial vehicle (UAV, e.g. balloons and helicopters) or a small all-terrain vehicle based laser scanning platform would be a promising development trend (Glennie *et al*. 2013). In this review, mobile laser scanning implies that a laser scanning system is deployed on the top of a land-based vehicle (Lemmens 2011). In the field of laser scanning, more terms, such as terrestrial mobile laser scanning (TMLS), land-based MLS or mobile LiDAR, are interchangeably used. Through this review, the term 'mobile LiDAR' is used.

Mobile LiDAR, a widely used technology since year 2003 when the first mobile LiDAR system emerged (Glennie 2009), has attracted much attention for mainly transportation-related applications (Jacobs 2005, Toth 2009, Stauth and Olsen 2013). It is a data revolution. With a mobile LiDAR system, mapping engineers can drive on a highway, rural road and railroad, or along the shoreline of a river or lake. Along the way, the system captures trees, bridges, streetlights, buildings, power lines and other street-scene small objects (e.g. cracks, road markings, etc.) in the form of 3D point clouds. In addition, the acquired 3D point clouds provide accurate 3D geospatial information of roadways. The collected data are a totally immersive 3D view of the objects and surroundings (Rybka 2011). Research achievements or application cases were demonstrated on various sources, such as conference presentations, peer-reviewed journals, industry magazines and websites, and technical reports (Williams *et al*. 2013). Thus, this review presents the results of an in-depth review of available literature to highlight the advancements of mobile LiDAR technology in road information inventory.

This review is important for researchers who are considering the use of mobile LiDAR technologies for road information inventory. The contents of this work include the following sections. First, the literature review presents background on the basis of mobile LiDAR technology, including in-depth descriptions of current mobile LiDAR system components, geo-referencing, error analysis and geometric accuracy validation. Next, this review shares insights on current and emerging road inventory applications of mobile LiDAR through academic research. Finally, a discussion of challenges and future research is presented and concluding remarks are given.

2. Mobile LiDAR technology

LiDAR technologies have become well-established surveying techniques for acquiring geospatial information because Global Navigation Satellite System (GNSS) technologies have been widely commercially used since the early 1990s (Beraldin *et al*. 2010). Closely followed by airborne LiDAR, terrestrial LiDAR (that is, the laser scanner is mounted on a tripod) and mobile LiDAR technologies have been rapidly developed. Mobile LiDAR

technology is being used at an increasing rate for transportation-related applications due to the following advantages. One of the crucial benefits of mobile LiDAR is its greater safety over other traditional surveying methods because mobile LiDAR performs road survey inside a vehicle with the flow of traffic, sparing surveyors the exposure to traffic and environmental hazards. Furthermore, mobile LiDAR efficiently performs road surveys with fewer surveyors at traffic speeds, day and night. In addition, mobile LiDAR collects a very wide range of data sets at various accuracies, from geographical information system (GIS) grade to survey grade (Gordon 2010). Therefore, a growing number of transportation agencies around the world have considered mobile LiDAR for road inventory and outlined corresponding guidelines for transportation-related applications (Williams *et al*. 2013). To fully picture the feasibility of mobile LiDAR for road surveys, this review will detail (1) its system configuration, (2) geo-referencing, (3) error analysis, and (4) geometric accuracy validation.

2.1. *System components*

Puente *et al*. (2013a) presented and compared several commercially produced mobile LiDAR systems. Though there are many types of mobile LiDAR systems, most mobile LiDAR systems consist of five essential parts: (1) a mobile platform; (2) a navigation solution system that integrates GNSS antenna(s), an Inertial Measurement Unit (IMU), and a wheel-mounted Distance Measurement Indicator (DMI); (3) laser scanner(s); (4) camera(s); and (5) a control system including data storages and integrating all sensors' function. In addition, a rigid platform firmly attaches laser scanners, digital cameras, GNSS and IMU, and other ancillary devices into a compact unit. The offsets between each sensor have to be strictly measured to remain stable for mobile LiDAR systems. Usually, these offset parameters are provided by the manufacturers; thus, no concerns of users are needed.

2.1.1. *Navigation sensors*

Among the navigation sensors, GNSS and IMU mainly provide accurate position and orientation measurements of a moving vehicle, and DMI provides supplementary positioning information during GNSS outage. Rather than one of these navigation sensors used alone, an integrated navigation system allows exploiting the complementary nature of these sensors. GNSS receivers provide three primary measurements: time, position and velocity (speed and direction). Position and velocity measurements are inputs to the logging computers and the IMU, respectively. Although GNSS receivers can provide highly accurate position information in an open environment, it suffers when satellite signals are blocked by high-rise buildings, vegetation, tunnels and other obstacles. On the other hand, IMU provides attitude information (e.g. roll, pitch and heading) of the moving vehicle, and requires no satellite signals to sense three-axis accelerations and three-axis angular rotations; however, the accuracy of position and orientation degrades with the time. An IMU sensor usually contains an embedded microcomputer unit and a module of accelerometers and gyroscopes. GNSS provides an initial IMU position and attitude, and thereafter the updated positions and velocities are calculated by integrating the measurements from the accelerometers and gyroscopes of IMU. Once IMU is initialised, no external information is required to determine its positions, velocities

and orientations; therefore, it is autonomous, immune to jamming or deception. IMU has almost no high-frequency errors but gives time-growing errors; while GNSS, on the other hand, has high-frequency noise but with good long-term accuracy. Thus, GNSS positions are augmented by IMU in periods of poor satellite conditions, while GNSS provides updated position information to IMU. Moreover, a wheel-mounted DMI constrains error drifts, especially during vehicle stoppages in areas of intermittent GNSS coverage. Attached to one of the vehicle's wheels, DMI measures wheel rotations, directly estimating a travelled distance. DMI usually supplements GNSS and IMU with additional positioning information. Wheel rotation data constrain drift, especially during vehicle's moving in areas of intermittent GNSS coverage. In addition, DMI assists in reducing duplicated LiDAR data while the vehicle is stopping.

2.1.2. *Laser sensors*

The number and arrangement pattern of laser scanners vary greatly with different mobile LiDAR systems. Laser scanners emit continuous laser beams at a fixed or user-defined angular increment to measure the distances to objects. In current mobile LiDAR systems, two techniques are mainly used for range measurements: pulse measurement and phase shift measurement (Beraldin *et al*. 2010, Lichti 2010). For pulse measurement (or time-of-flight (TOF)), a laser scanner emits pulse beams and records the round-trip time to and back from the measured objects to measure the range based on the light propagation velocity in a given medium.

Phase measurement in continuous wave modulation can be considered as an indirect form of TOF measurement. Continuous waves can be modulated in amplitude modulation (AM) or frequency modulation (FM) for measuring target ranges. Amplitude modulation measures the range using phase difference between the emitted laser beam and the returned laser light. Frequency modulation measures the range by exploiting beat frequencies (Beraldin *et al*. 2010).

Generally, the phase shift mode tends to have very high data rates (up to 1,000,000 points/s) and higher precision ranging from sub-millimetre to sub-centimetre, but shorter measuring ranges (<100 m) (Petrie and Toth 2008, Beraldin *et al*. 2010). On the contrary, the TOF measurement has a much longer range (e.g. 800 m) but lower data rates (usually <500,000 points/s in TLS (terrestrial laser scanning) /mobile LiDAR and <20,000 points/s in ALS (airborne laser scanning)) and relatively lower precisions ranging from sub-centimetre to centimetre level. The TOF mode is commonly used for the majority of current commercially available mobile LiDAR systems, while the phase mode is mostly used for terrestrial LiDAR systems. Examples of TOF laser scanners include Velodyne (2016), Optech Lynx (2016), RIEGL (2016), Sick (2016), Leica (2016), Trimble (2016), and DYNASCAN MDL (2016). Examples of phase shift laser scanners include Z+F (2016) and Faro (2016). FARO and Z+F scanners have also been operated in mobile LiDAR systems. Many types of TOF-based and phase-based laser scanners in mobile LiDAR systems are set to operate in a 2D scan line /planar mode, while the third dimension of the acquired 2D scan data can be obtained by the forward movement of the vehicle.

The quality of a laser scanner is determined by the following factors: eye safety, accuracy, field-of-view, data rate, scan frequency and range (Iavarone 2007). Table 1 lists the system parameters of several laser scanners popularly used in the market. Laser scanners use Class 1 eye safety rating, that is, the beam is invisible and safe to human

Table 1. System parameters of several currently popularly used laser scanners.

Laser scanner	SICK LMS 291	MDL LMS511	RIEGL VQ-450	Optech Lynx SG1	Z + F PROFILE 9012	Faro Focus x330	Velodyne HD64
Data rate (kHz)	40	36	550	150–1200	1000	976	1333
Scan rate (Hz)	75–100	25–100	200	500	200	97	5–15
FOV (°)	180(H)/ 90(V)	190	360	360	360	360(H)/300(V)	360 (H)/26.8(V)
Range (m)	80 (10% reflectivity)	40 (10% reflectivity)	800 (80 reflectivity)/ 70 (10 reflectivity)	250 (10 reflectivity)	119	0.6–330	120 (80 reflectivity)/ 50 (10 reflectivity)
Range precision (mm)	10 mm @1-20 m		5	5	1	1	10
Range accuracy (mm)	± 35	± 10 @ 50 m	8	±50	1	±2	<50
Returns (#)	–	5	Practically unlimited	4	1	1	1
Laser type	TOF	TOF	TOF	TOF	Phase	Phase	TOF

eyes in both aided and unaided conditions. The accuracy of a mobile LiDAR system directly determines the accuracy of the final deliverable products. A field-of-view dictates the extent of the area that can be covered in a single pass of the collection vehicle. The laser scan rate and data rate determine mobile LiDAR data collection rate. As shown in Table 1, RIEGL VQ-450, one of the most advanced commercially available laser scanners, has a scan rate of up to 500 Hz, which allows the users to collect highly accurate data of required ground point density within a very short period of time. The point resolution of the collected data depends on several factors, including vehicle speed, laser mirror scanning speed and system measurement rate.

2.1.3. *Camera/video recording*

Most mobile LiDAR systems incorporate camera(s) to provide ancillary information. For example, for visualisation, the points collected by laser scanners can be colourised by true-colour information in the real world. Similarly to laser scanners, the number and arrangement pattern of digital cameras vary with different mobile LiDAR systems. Different mobile LiDAR systems configure different numbers of digital cameras in many deployed patterns. For example, a typical Trimble MX-8 system is deployed with four Grasshopper ® GRAS-50S5C CCD cameras with a maximum resolution of 2448 × 2048 pixels and a maximum frames per second of 15. The VMX-450 mobile LiDAR system is typically configured with four digital cameras, each of which is sealed with a protective housing for operating under different environmental conditions. The specific deployment of cameras is customised by users and projects. This additional colour information contributes to road feature extraction because it provides a great level of features details.

2.2. *Direct geo-referencing*

Calculating ground coordinates for illuminated objects, termed 'geo-referencing', from a mobile LiDAR system can be found in the literature (Glennie 2007). The laser scanner is referenced when its position and orientation relative to the mapping coordinate system is known by a set of navigation systems. The navigation data must be precisely time stamped for sensor integration and determination of the exact coordinates of mapping points (Barber *et al*. 2008). The coordinates of a target *P* shown as Figure 1 can be calculated by

$$\begin{bmatrix} X_P \\ Y_P \\ Z_P \end{bmatrix}^M = \begin{bmatrix} X_{GNSS} \\ Y_{GNSS} \\ Z_{GNSS} \end{bmatrix}^M + R^M_{IMU}(\omega,\varphi,\kappa)\cdot\left(R_S^{IMU}(\Delta\omega,\Delta\varphi,\Delta\kappa)\cdot r_P^S(ad) + \begin{bmatrix} L_X \\ L_Y \\ L_Z \end{bmatrix}_S^{IMU} - \begin{bmatrix} L_X^{\frac{G}{T}} \\ L_Y^{\frac{G}{T}} \\ L_Z^{\frac{G}{T}} \end{bmatrix}_{GNSS}^{IMU} \right) \tag{1}$$

where the parameters in Equation (1) are listed in Table 2. Equation (1) defines the relationship among all observation parameters for producing geo-referenced point clouds.

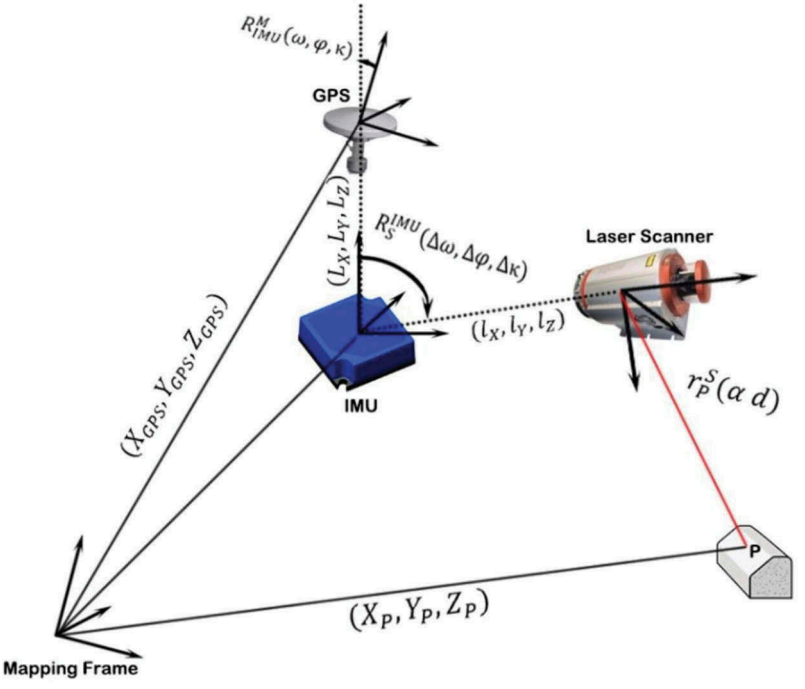

Figure 1. An illustration of coordinates between mapping frame, target and mobile LiDAR system.

Table 2. Parameters used in geo-referencing.

X_P, Y_P, Z_P	Location of the target P in the mapping frame.
$X_{GNSS}, Y_{GNSS}, Z_{GNSS}$	Location of GNSS antenna in the mapping frame.
$R^{M}_{IMU}(\omega, \varphi, \kappa)$	Rotation matrix between IMU and mapping frame, $(\omega, \varphi, \kappa)$are the roll, pitch and yaw of the sensor with respect to the local mapping frame. These values are provided by the IMU system.
$R^{IMU}_{S}(\Delta\omega, \Delta\varphi, \Delta\kappa)$	Rotation matrix between the laser scanner and IMU, $(\Delta\omega, \Delta\varphi, \Delta\kappa)$ are the boresight angles which align the scanner frame with IMU's body frame. Those values are determined by the system calibration.
$r^{S}_{P}(ad)$	Relative position vector of Point P in the laser scanner coordinate system, a and d for scan angle and range measured and returned by the laser scanner.
$L_X, L_Y L_Z$	Lever-arm offsets from the navigation and IMU origin to the laser scanner origin. These values are determined by system calibration or measurement.
$L_X^{(G/I)}, L_Y^{(G/I)}, L_Z^{G/I}$	Lever-arm offsets from the IMU origin to the GNSS origin. These values are determined by system calibration or measurement.

2.3. *Error analysis for mobile LiDAR systems*

Equation (1) defines the relationship among all observation parameters for producing geo-referenced point clouds. To examine the final point accuracy, we discuss the following typical errors of these observations.

Laser scanner errors: According to Equation (1), the factors that influence the coordinates of point *P* include distance error (Δd) and scanning angle error ($\Delta\alpha$). The error in distance is caused by the internal accuracy of the clock that measures the time of flight and the width of the output laser pulse; the error in scanning angle is due to the angular resolution of the laser scanner angle encoder and the uncertainty of beam divergence (Olsen *et al*. 2013).

IMU attitude errors: The IMU component of a mobile LiDAR system provides roll, pitch and heading angles that represent the rotation relationship between the IMU and the mapping frames. An IMU consists of two main parts: (1) three orthogonal accelerometers, each of which measures the acceleration along a specific axis, and (2) three orthogonal gyroscopes, each of which measures and maintains the orientation, based on the principles of conservation of angular momentum. Accordingly, systematic errors of the sensor include accelerometer biases and gyro drifts. Typically, as IMU components are supplied by two or three different system manufacturers, their accuracies can be examined from the manufactures' technical specifications. For example, RIEGL VMX-450 is configured with a set of Applanix® POS LV 510, whose typical accuracy can be found on the manufacturer's technical specification (http://www.applanix.com). Applanix® POS LV 510 can deliver 0.005° in roll and pitch, and 0.015° in heading (at 1σ).

Positioning errors: The positioning accuracy of a GNSS subsystem is influenced by the following factors: multipath, atmospheric errors, baseline length, poor satellite geometry and loss of lock (Haala *et al*. 2008); therefore, the absolute level of the positioning accuracy for mobile LiDAR survey is difficult to quantify. Ideally, the positioning accuracy is expected to be 1 cm +1 ppm horizontally and 2 cm +1 ppm vertically within a relatively short kinematic baseline (<30 km) (Bruton 2000).

Lever-arm offset errors: Usually, the origins of laser scanners and IMU cannot be collocated; the lever-arm offsets thus must be known in order to obtain accurately georeferenced mobile LiDAR point clouds. There are two methods to measure the lever-arm offsets: calibration and physical measurement. Compared with the first method, the second one is widely used because it is simple to implement. Accordingly, the measurement errors are also introduced because of the assumption of the alignment of two sensors' axes (Glennie 2007, Olsen *et al*. 2013).

Boresight errors: The boresight errors result from the misalignments between the IMU and laser scanner measurement axes, as shown in Figure 1. To process laser scanning data, the location of the scanner and its orientation in relation to the IMU must be precisely known because alignment errors will be propagated over the distance between the sensor and the object being scanned. Boresighting is a very precise measurement process that attempts to correct any mounting misalignments between the IMU and laser scanners (Rieger *et al*. 2010, Lim *et al*. 2013).

The above discussion of error sources for a mobile LiDAR system demonstrates that the accuracy of mobile LiDAR point clouds depends on the underlying accuracy of GNSS/IMU and laser scanners. Among those errors, two possible error sources (boresight and lever-arm) can be recovered by system calibration. In fact, the overall accuracy of mobile LiDAR point clouds is mainly affected by the navigation solution because of multi-path effects and signal shading that are caused by high-rise buildings and trees along the street deteriorate GNSS conditions in a moving vehicle (Barber *et al*. 2008, Haala *et al*. 2008). Compared to a long distance from an aircraft to the ground in ALS, GNSS positioning errors of a mobile LiDAR system have a much greater impact on the overall error budget, owing to a short distance between a laser scanner and a scanned object, even about several to 10 metres. To improve mobile LiDAR data accuracy, a post-processing procedure of navigation trajectory is indispensable.

2.4. *Geometric accuracy validation*

As mentioned above, mobile LiDAR systems must operate different sensors (i.e. GNSS, IMU, DMI and laser scanner) to provide geometric quantities, and synthesise these quantities to detail point cloud data. To ensure that engineers and decision-makers take full advantage of using mobile LiDAR technology, accuracy verification must be conducted because mobile LiDAR systems have their own set of limitations and their performance vary with some factors, such as range distance, object reflectivity, incident angle of laser pulse to the reflective object, and the accuracy of navigating system. A literature review is presented to report such geometric validation work.

Goulette *et al*. (2008) reported that the laser-based LARA-3D system produced an estimated measurement precision of 5 cm. Barber *et al*. (2008) conducted geometric validation of a Streetmapper system (integrated with the TERRA control GPS/IMU system and three Riegl laser profilers). The experiments assessed the precision and accuracy of delivered data across two test sites: a peri-urban residential housing estate with low-density housing and wide streets, and a former industrial area containing narrow streets and tall warehouses. The study showed that a measurement precision (95%) of between 2.9 and 3.1 cm was achieved in elevation; RMS errors in elevation were in the order of 3 cm; the planimetric accuracy of approximately 10 cm was achieved. The experimental results demonstrated that the system can be successfully used in the survey of urban areas. Puente *et al*. (2013b) assessed the performance of a Lynx Mobile Mapping system from Optech Inc. The system was operated at a maximum scan frequency of 200 Hz, pulse repetition frequency of 500 kHz per sensor, and a scanning field of view of 360°. Absolute accuracy levels around 1–5 cm and a relative accuracy level of 10 mm were achieved, which made the system suitable for very accurate applications.

Lim *et al*. (2013) assessed the vertical and horizontal accuracies of data collected by the mobile LiDAR system, including an Optech ILRIS 3DMC laser scanner, and the navigation instruments (an IMU and two GPS antennas). The final point cloud accuracy was 6.0 cm (east), 9.5 cm (north) and 5.3 cm (height). The study also demonstrated that the point-to-point spacing in a single scan line varied from 2 to 5 cm at the ranging distance of <30 m and the minimum scan line spacing of 10 cm was observed at a vehicle speed of 8 km hour^{-1}, a scan angle of 10° and a scan count of 80.

Guan *et al*. (2013) assessed the performance of Trimble MX-8. The system configuration is detailed in Figure 2. Two survey areas were within Fengtai District, northwest of Beijing, China. The first test site was a two-side, four-lane road with a greenbelt in the middle. Many residential buildings (about 5 or 6 storeys) and large industrial manufactories and warehouses were interspaced along the sides of the road. The sky view across the street was considered as a good case for capturing more GPS signals although a small amount of overhanging vegetation that restricted visibility was located along the street. The second test site was relatively narrow and approximately 26.9 km long. More high-rise commercial buildings and apartments were located along the survey route. The city canyon was created by narrow streets and high-rise buildings, which limited the sky view for capturing satellite signals. In addition, there was a high bridge crossing the pass, further blocking the satellite signals.

To validate the performance of the system in Guan *et al*. (2013), around 30 control points (corner points of objects on the streets and white road markings) for validation

Figure 2. A system configuration of a Trimble MX-8. The system includes two Riegl® VQ-250 laser scanners, four Point Gray Grasshopper ® GRAS-50S5C CCD cameras, and a set of navigation system containing two GNSS antennas, an IMU, and a DMI. (Guan *et al*. 2013).

were collected for each test site. The mean standard deviations of planimetric accuracy for the left and right laser scanners were 4.2 and 3.3 cm, respectively. The mean standard deviations of vertical accuracy for the two laser scanners were 1.7 and 2.1 cm, respectively. Notice that the minimum standard deviation appeared at the check points measured near the base station with a good GPS coverage. In spite of errors of check points, the accuracy of mobile LiDAR points was still consistent to the accuracy of the navigation system and even outperforms the Applanix's specification. The errors were lower than ±5 cm, and met the requirements of data accuracy for urban surveying.

Assuming that a road within a small local area was flat, road data within a small rectangle were selected to calculate the elevation precision. The local precision was determined by evaluating the residuals following a least square of the mobile LiDAR points to the plane. For example, the yellow points shown in Figure 3(a) were fitted to a plane and individually calculated the distance to the plane based on the plane parameters. As shown in Figure 3(a), the minimum standard deviation was 1.477 mm, and the maximum standard deviation was close to 2 mm. Similarly, the data on a vertical advertising board attached to a light pole were selected for the assessment of planimetric precision of the collected point clouds, as shown by the yellow points in Figure 3(b). Compared to the elevation precision, the planimetric precision was a little lower; the standard deviation ranged from around 7 to 11 mm. For common transportation applications, the 3D accuracy at 95% confidence generally required a range of 1 cm (e.g. engineering survey, DEM, pavement survey and slope stability) to 10 cm (e.g. urban

Figure 3. Precision of the collected mobile LiDAR points, (a) vertical, and (b) planimetric.

modelling and roadway condition assessment) based on the information from literature review, questionnaire and project team experience. Thus, this geometric validation demonstrated that the data collected by a Trimble MX-8 system were sufficient for the transportation-related road features in both horizontal and vertical precision.

3. Main road inventory applications

Duffell and Rudrum (2005) discussed that a point cloud can be utilised to perform road inventory mapping, including any road-scene structure, road pavement, traffic signalling devices, etc. (Williams *et al*. 2013, Landa and Prochazka 2014). According to Landa and Prochazka (2014), mobile LiDAR data can be used for different types of road-scene object inventory, which can be subdivided into three types: road pavement, road surface structures (e.g. road markings and road cracks), and pole-like objects (e.g. light poles and traffic signposts). This article will focus on the aforementioned three types of road-scene objects. Other objects such as trees, buildings, vegetation and powerlines will be excluded from this article.

3.1. *Road pavement extraction*

Although geometric design parameters for recently built roads are mostly available, these data for old roads are unavailable or unusable for upgrading or assessing the quality of the roads (Jaakkola *et al*. 2008). When interpreting mobile LiDAR point clouds, different road detection/extraction algorithms were developed. These algorithms are categorised into five groups, in terms of (1) road geometric shape, (2) the use of road geometric features and LiDAR data characteristics, (3) data format, (4) the use of classification methods, and (5) external data sources. Accordingly, the following subsections will comprehensively detail the literature.

3.1.1. *Identifying 3D road surface points by road structure representation*

Some algorithms directly detected planar road surfaces, while the others extracted roads by first detecting and fitting linear road edges. The direct extraction of planar road surfaces are performed by model fitting methods, such as Hough Transform (Takashi and Kiyokazu 2006), RANSAC (Smadja *et al*. 2010), and weighted least-squares linear fitting

(Yuan *et al*. 2010). By using Hough Transform, Takashi and Kiyokazu (2006) directly identified road lanes with curvature, yaw angles and offsets derived from point clouds. However, applying Hough Transform to large volumes of mobile LiDAR data is quite time consuming and computationally intensive. Yuan *et al*. (2010) employed a fuzzy clustering method based on maximum entropy theory to segment points, followed by a multi-time weight least-squares linear fitting algorithm to differentiate linearly and nonlinearly distributed point segments. Similarly, these methods, which require intensive computations to extract roads from mobile LiDAR data, are time consuming. Smadja *et al*. (2010) suggested a two-step road-surface extraction algorithm based on local road shape. RANSAC was first applied to each scan line individually for roughly estimating road sides. Then, the curb candidates were picked out by a multi-frame accumulated map for road extraction.

To improve computational efficiency, many studies extract roads by detecting and extracting road edges (Goulette *et al*. 2008, Yoon and Crane 2009, McElhinney *et al*. 2010, Ibrahim and Lichti 2012, Kumar *et al*. 2013, Yang *et al*. 2013). Yoon and Crane (2009) estimated road edges by using two criteria: slope and standard deviation calculated from mobile LiDAR points. McElhinney *et al*. (2010) proposed a two-step strategy: (1) generation of a set of lines from points, and (2) extraction of road edges according to slope, intensity, pulse width and proximity to vehicle information. Ibrahim and Lichti (2012) extracted curb edges by applying the derivatives of the Gaussian function to mobile LiDAR points. Based on elevation difference, point density and slope changes, Yang *et al*. (2013) modelled three types of curbs with a moving window operator.

3.1.2. *Identifying 3D road surface points or point clusters using data characteristics and road properties*

In this category, some road detection and extraction algorithms are developed by using different LiDAR data characteristics (e.g. point density and intensity), road properties (e.g. curb, minimal road width and elevation), and their combinations. Given the mobile LiDAR scanning mechanism, point density is inversely proportional to the scanning distance from the mobile vehicle's trajectory. By analysing varying point densities, Ibrahim and Lichti (2012) separated ground points from non-ground points. Other data characteristics include local point patterns, intensity and pulse return information (e.g. pulse width and scanning angular coordinates), height, and height-derived information (e.g. slope, height variance, mean value and height differences). In most cases, several characteristics of a LiDAR point cloud were combined to segment road points from the entire scanned LiDAR data (Jaakkola *et al*. 2008, Munoz *et al*. 2008, Yoon and Crane 2009, McElhinney *et al*. 2010, Pu *et al*. 2011, Wang *et al*. 2012, Kumar *et al*. 2013, Fan *et al*. 2014, Hata *et al*. 2014). In addition, a prior knowledge of the road of interest was widely used in the literature. Road features include curb, minimal road width and elevation information. Guo *et al*. (2015) combined road width with the elevation data of point clouds to filter out non-road surface points. Curbs are a critical feature for road extraction because curbs represent boundaries of roads in an urban environment. As mentioned, some studies extracted road edges by identifying curbs (Yang *et al*. 2013, Guan *et al*. 2014a).

3.1.3. *Identifying road surfaces from 3D raw point clouds or 2D feature images*

Road extraction can be performed on either 3D LiDAR points (including 2D scan profiles) or 2D feature images interpreted from 3D points. Along every direction and orthogonal direction of the scan line segment between two adjacent trajectory points, Wang *et al*. (2012) iteratively detected road surfaces and boundaries based on a height threshold, altitude variance and altitude mean value. Hata *et al*. (2014) extracted roads by applying differential, distance and regression filters to 3D raw LiDAR points. To decrease computational cost, trajectory data were intuitively used (Ibrahim and Lichti 2012, Wang *et al*. 2012, Guan *et al*. 2014a). As reviewed, mobile LiDAR systems acquire data scan line by scan line. The spatial configuration of the scan lines depends on the setting parameters of a system, i.e. speed of the vehicle, sensor trajectory, scanner orientation, and sensor measurement and rotation rates. The greater point density of road surface points permits a computational improvement in road extraction by processing scan lines (Manandhar and Shibasaki 2001, 2002, Zhao and Shibasaki 2002, Yang *et al*. 2013, Guan *et al*. 2014a). Manandhar and Shibasaki (2001) relied on the information from individual scan lines to classify points into roads and buildings. Based on scan lines, Zhao and Shibasaki (2002) first classified range points into the groups of vertical building surface, road surface, other surface, window, tree and unknown objects. Then, an erroneous measurement was implemented to record irregular data in the window areas. Volumetric modelling and marching cube method were exploited to model both surface-structured objects, e.g. building and road surfaces, and volume-structured objects, e.g. trees.

Several studies first segmented 3D points into line sections, on which laser data features and road properties were analysed to obtain road information (Abuhadrous *et al*. 2004, McElhinney *et al*. 2010, Cabo *et al*. 2015, Riveiro *et al*. 2015). Abuhadrous *et al*. (2004) classified points into buildings, roads and trees by analysing two histograms in the Z- and Y-directions in one profile to reflect the horizontal or vertical nature of urban targets.

Converting 3D points into 2D feature images is an effective way to extract road surfaces from large volumes of mobile LiDAR data (Hernandez and Marcotegui 2009). By using the established image processing algorithms, road edges or road surfaces can be detected and extracted efficiently. Kumar *et al*. (2013) applied a combination of two modified versions of the parametric active contour or snake model to 2D elevation, reflectance and pulse width raster data, which were interpreted from the first-level terrain pyramids using natural neighbourhood interpolation.

3.1.4. *Identifying road surfaces by using road-scene classification approaches*

Some algorithms focus on a specific road-scene object, while others prefer to classify the whole scene into different types of objects of interest at one time. With a mobile LiDAR system, the collected data are a totally immersive 3D view of the objects and surroundings (Rybka 2011). Different authors proposed a plenty of automated or semi-automated algorithms to recognise different road features within a point cloud at one time, such as traffic signposts, trees, building facades, road surfaces and road markings (Jaakkola *et al*. 2008, Munoz *et al*. 2008, Shen *et al*. 2008, Pu *et al*. 2011, Fan *et al*. 2014, Díaz-Vilariño *et al*. 2016).

Considering geometrical characteristics (e.g. linear structures, planar structures, free shapes whose projections onto the ground have a specific width), Goulette *et al*. (2008)

segmented point clouds into two groups: one group containing grounds and roads, while the other group including facades and trees. Munoz *et al*. (2008) described an Associative Markov Network (AMN) to roughly classify point clouds of urban road environments. Then, local point distribution was proposed to label points as linear, planar or scatter structures. Finally, the post-processing step using height histogram and surface fitting was performed to obtain five classes (e.g. vegetation, wires, poles, load bearings and façades). The overall classification rate was around 90%. Fan *et al*. (2014) classified a point cloud into six classes (e.g. buildings, roads, vehicles, trees, poles and traffic signs) based on height histogram, point density and regular geometric features. Pu *et al*. (2011), by using size, shape, orientation and topological relationships, automatically extracted ground surface, objects on ground and objects off ground (e.g. traffic signs, trees, building walls and barriers) within a point cloud. The authors mentioned an 86% accuracy of pole detection and pointed out that images were required for extraction.

3.1.5. *Extracting road surfaces by fusing with other data sources*

Such as video cameras (Yu *et al*. 2007) and airborne laser scanning data (Boyko and Funkhouser 2011). Yu *et al*. (2007) created 3D surface geometric models from mobile LiDAR data with fine geometric details of cracks that are only a few centimetres wide along with the depth information. The authors claimed that the entire process required minimal human intervention in tuning parameters. With higher resolution 2D texture information, road objects, such as road distresses, were archived and analysed. To overcome the challenges that the points from different scanners may be captured at different times, in different weather conditions, under different illuminations and with different sampling densities, Boyko and Funkhouser (2011) proposed a method for extracting roads from a large-scale dense point cloud merged from multiple aerial and terrestrial source scans of an urban environment. Registered the given 2D map of a road network with the input 3D point clouds, a map spline was first created and then split into independent parts, road patches. Accordingly, a sub-cloud of relevant points for each road patch was calculated to a ribbon snake by optimising an active contour that aims to maintain the smoothness of its boundary while fitting its boundary to likely predictions in the attractor map. Finally, for each individual sub-cloud, the points that fall inside the active contour were labelled road points.

3.2. *Road surface structures*

Recently, mobile LiDAR intensity data have been explored to detect other road-surface features, such as highly reflective road markings (Jaakkola *et al*. 2008, Toth *et al*. 2008; Vosselman 2009, Smadja *et al*. 2010, Yang *et al*. 2012a, Guan *et al*. 2014a) and even illuminated structures (e.g. manholes and sewer wells (Yu *et al*. 2014a, 2015c), tunnels and culverts (Puente *et al*. 2014, Lin and Hyyppä 2010).

Road markings on paved roadways, as critical features in traffic management systems, have important functions in providing guidance and information to drivers and pedestrians. For example, driver-assistance systems require reliable environmental perception to improve traffic safety by informing motorists and preventing accidents. Along with pavement condition and road topography, the visibility of road markings is a key element in

accidents where the road itself is the cause. Especially, in highly populated urban environments, high accident rates are caused by the absence of clearly presented road signals (Carnaby 2005). Road markings are highly retro-reflective surfaces painted on roads; reflectance of the target in the form of intensity can be used to identify road markings (Chen *et al*. 2009, Mancini *et al*. 2012, Guo *et al*. 2015, Riveiro *et al*. 2015).

Most researchers segmented road markings from 2D feature images converted from 3D points. Based on semantic knowledge (e.g. shape and size) of road markings (Yang *et al*. 2012b), the established image processing algorithms were applied, such as thresholding-based segmentation, Hough Transform, morphology and Multi-Scale Tensor Voting (MSTV) (Jaakkola *et al*. 2008, Chen *et al*. 2009, Vosselman 2009, Smadja *et al*. 2010, Mancini *et al*. 2012, Guo *et al*. 2015, Riveiro *et al*. 2015, Guan *et al*. 2015b). The use of Hough transformation for road marking extraction is weakened by specifying the number of road markings to be detected, which is a limiting factor for complex types of road markings such as hatchings and words. To overcome intensity inconsistency caused by scanning pattern, multiple thresholding methods were researched by defining the relationship between scanning distances with intensity values (Vosselman 2009, Guan *et al*. 2014a). Guan *et al*. (2014a) dynamically extracted road markings with multiple thresholds that corresponded to different ranges determined by appropriate point-density normality, followed by a morphological closing operation with a linear structuring element. The extracted road markings are shown in Figure 4. Guan *et al*. (2015b) achieved a further improvement in road marking extraction by using multi-scale tensor voting (MSTV). The MSTV algorithm had an advanced capability to efficiently suppress high-level noise and infer perceptual structures from noisy or corrupted data. Yu *et al*. (2015a) emphasised an automated road marking extraction from 3D mobile LiDAR point clouds rather than the derived feature images. After road marking segmentation, the

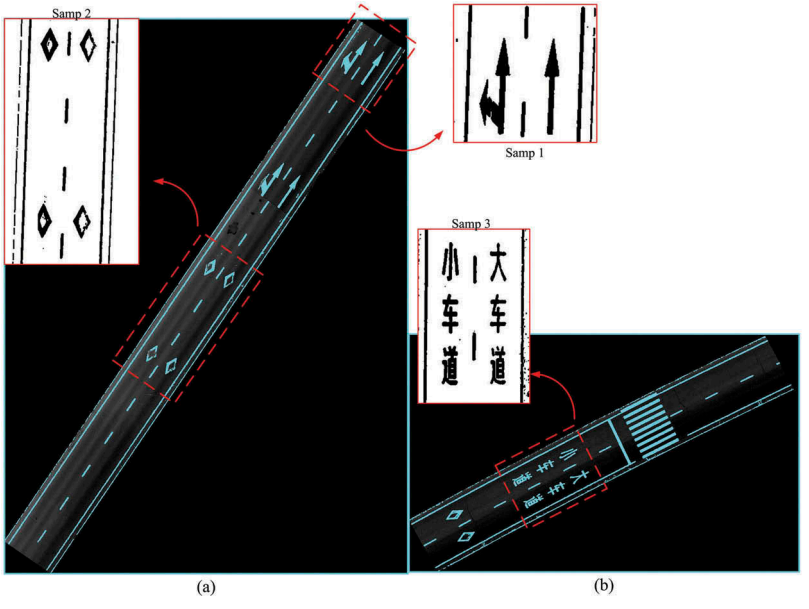

Figure 4. The extracted road markings overlaid on the geo-referenced intensity images: (a) Huandao and (b) ICEC data sets (Guan *et al*. 2014a).

authors dealt with large-size markings based on trajectory and curb-lines, and small-size markings based on deep learning and principal component analysis (PCA). Within point clouds, the authors finally classified road markings into boundary lines, stop lines, rectangular markings, pedestrian markings, arrow markings, zebra crossing lines and centrelines.

Pavement manholes provide access to conduits that are used to conduct rainwater, drainage, steam, natural gas and other utility networks including telecommunication wires and power cables. It is one of the key elements in urban environment that ensures quality of life, economic prosperity and national security (Pikus 2006). Manholes are usually covered with metal or concrete covers, resulting in the retro-reflective differences between manhole covers and road surfaces in the near-infrared spectrum. Due to manhole covers being located on road surfaces, several manhole cover extraction algorithms were performed on 2D raster data interpolated from 3D mobile LiDAR points. Guan *et al*. (2014b) extracted manhole covers by applying distance-dependent thresholding, multi-scale tensor voting and morphological operations to the interpolated feature images. Similarly, Yu *et al*. (2015c) developed a supervised deep learning model to depict high-order features of local image patches, and a random forest model to locate urban road manhole covers. In Yu *et al*. (2014a), marked point processes were proposed to detect circular-shaped and rectangular-shaped manhole covers from mobile LiDAR point clouds. To further precisely locate manhole covers, Ji *et al*. (2012) developed a new method combined with multi-view matching and feature extraction techniques by using close-range images and mobile LiDAR data.

In addition to providing a high promising solution to the extraction of road markings and manhole covers, mobile LiDAR data might be a valuable data source for estimating pavement distresses, which can be caused by fractures due to excessive loading, fatigue, thermal changes, moisture damage, slippage or contraction. Based on the visual appearance of cracks in the near-infrared range usually darker than that of the normal road surface, Guan *et al*. (2015a), developed a multi-scale tensor voting (MSTV) strategy to extract curvilinear pavement cracks. The authors indicated that pavement cracks were recognised with the average scoring measure (SM) value of 91.5.

3.3. *Pole-like objects*

Utility poles, traffic signs and lamp posts can be considered as an important part of road infrastructure. Mobile LiDAR technology has been widely used to detect these pole-like objects and tree trunks (Manandhar and Shibasaki 2001, Chen *et al*. 2007, Hofmann and Brenner 2009, Jaakkola *et al*. 2010, Lehtomäki *et al*. 2010, Yokoyama *et al*. 2013).

Based on eigenvalue analysis, principal component analysis (PCA) was a widely used method for detecting pole-like objects from irregular point clouds (Yokoyama *et al*. 2011, 2013). These PCA-based methods detect linear pole-like structures by first constructing a covariance matrix for each point with its neighbours and then analysing eigenvalues decomposed from the covariance matrix (El-Halawany and Lichti 2011). Eigenvalue-based PCA methods show high computational efficiency. However, other objects (particularly tree trunks) in a road scene might cause a considerable number of false alarms.

Traffic signs in point clouds are shown by retro-reflectively painted planar objects. Chen *et al*. (2009) explored intensity information of mobile LiDAR data to detect traffic signs and lane markings. The intensity is a measure of the retro-reflectivity property of the scanned surfaces (Riveiro *et al*. 2016).

Shape and context features were also widely used in pole-like object detection methods (Teo and Chie 2016). Shape features were characterised based on height, number and types of attached part segments (Yang and Dong 2013); whereas context features were computed based on surrounding distributions (Yokoyama *et al*. 2013, Yu *et al*. 2014b). For example, in Yu *et al*. (2015b), a pairwise 3D shape context descriptor, which considered both local and global similarity measures, was proposed to detect light poles. Pole-like objects in 3D mobile LiDAR point clouds show circular-shaped structures at the top-down view. Therefore, point clouds are horizontally sectioned into a number of profiles, on each of which approximate circles or eclipses are detected as pole-like candidates. Kukko *et al*. (2009) and Lehtomäki *et al*. (2010) clustered scan lines in a local neighbourhood to detect pole-like objects profile by profile. Brenner (2009a, 2009b) investigated local upright patterns and *Z*-directional extension of a pole, and then extracted the pole structures in stacks of hollow cylinders. Pu *et al*. (2011) developed a percentile-based method with respect to shape, height and size of light poles. Puttonen *et al*. (2013) integrated a different distance sensitive sampling method into the method proposed by Lehtomäki *et al*. (2010). With the prior knowledge of pole-like objects in shape and size, by using grammar rules, a voxel structure (that is a volumetric cubic unit) was applied to mobile LiDAR data (Cabo *et al*. 2014). For each voxel, Cabo *et al*. (2014) considered only the coordinates of the centroids and the number of points to reduce the original point cloud. After voxelisation, 2D analysis was performed by the following three stages: (1) segmentation of the connected horizontal elements, (2) selection of elements by a maximum area criterion and (3) selection of elements by an isolation criterion. Finally, a 3D neighbourhood analysis was used to detect pole-like street furniture objects. Pole-like objects were extracted by analysing scan lines, rather than raw point clouds (Chen *et al*. 2007, Kukko *et al*. 2009, Lehtomäki *et al*. 2010, Hu *et al*. 2011). Manandhar and Shibasaki (2001) detected vertical poles by extracting vertical line segments from individual scan lines. To improve computational efficiency, some studies were performed on 2D feature images (El-Halawany and Lichti 2013). Point density in 2D feature images was also exploited to detect light poles (Chen *et al*. 2007).

Moreover, mobile LiDAR systems can provide high-density point clouds at a normal vehicle speed. In the vertical direction, pole-like objects contain more points than other objects such as road surfaces (Yan *et al*. 2016). Golovinskiy *et al*. (2009) presented a step-wise urban feature (including poles) recognition method. First, point density was explored to select potential objects. Next, the candidate objects were separated from the background, and they were characterised according to their spatial context and configuration. Finally, the features were classified by comparing their characterisation with the labelled data from a training data set.

4. Current challenges and future trend

The literature review reveals that Mobile LiDAR offers a huge potential for road information inventory, mainly due to its improved safety, efficiency, flexibility and data

reusability. More importantly, mobile LiDAR, as an active remote-sensing technology, provides highly accurate point clouds with high point density. However, several challenges exist when implementing mobile LiDAR data in road-related applications. Future trends will emerge accordingly.

Although mobile LiDAR has been commercially available for one decade, few standards have been developed when using mobile LiDAR for carrying out road inspections along the route corridor. Thus, in the foreseeable future, a consistent guideline is urgently required to standardise the adoption of mobile LiDAR by transportation agencies. Standards and best practices, such as control requirements, accuracy standards, data interoperability and management, and data quality needs of specific applications, will be established and developed for various road inventory-related applications. As a result, experienced geomatics personnel can be involved throughout the entire process when using mobile LiDAR technology for road inventory.

Note that mobile LiDAR technology will certainly not replace current conventional methods of topographic data collection. The mobile LiDAR data, in most cases, may need to be supplemented by data collected from conventional surveying, GNSS, aerial /UAV photogrammetry and airborne LiDAR (Gordon 2010). Accordingly, integration of mobile LiDAR data with other data sources for road inventory is greatly needed to use the complementary characteristics of these data sets.

The data set size and data complexity are considered as significant challenges. Hardware manufactures continue to build advanced mobile LiDAR systems. For example, the RIEGL VMX-250 system, which can collect 0.5 million points per second, was developed into the current RIEGL VMX-450 system that collects 1.1 million points per second. A RIEGL VMX-250 system collects data up to a total of 120 Gigabytes (including 40 Gigabytes image files and 80 Gigabytes LiDAR point clouds) in one hour at the speed of 40–45 km/h. The size and complexity of mobile LiDAR data require upgrading not only the entire computing infrastructure (software, workstations, servers, data storage and network backbone) but also data post-processing packages for road-information extraction. Data post-processing is the key to a complete solution for the end-users (e.g. transportation engineers/agencies) because they are less interested in the actual point cloud data than in the computer-aided model (CAD) formatted geometric road information. Manually processing large volumes of mobile LiDAR data for road-information extraction is very time consuming. To process the entire data set efficiently, most current software packages adopt the common strategy, where the data are subsampled or segmented into small tiles/sections. In addition, the majority of existing methods developed for performing road inventory are of high computational complexity. Effective object recognition methods will be required to perform road geometry and road physical data in a timely manner. Furthermore, considering the object recognition in mobile LiDAR data, multiple attributes including elevation, intensity pulse width, range, incident angle and multiple echo information can be explored for extracting road features.

Currently, the advanced third-party point-cloud post-processing software includes Leica Cyclone®, InnovMetric PolyWorks®, GeoCue software suite, TerraSolid software suite, PHOCAD PHIDIAS®, Bentley Pointools, and Virtual Geomatics software suite (Yen *et al*. 2011). Most third-party software packages deal with small volumes of 3D points or involve one or several steps when processing mobile LiDAR data. Multiple software packages have to work together to obtain the CAD-formatted deliverables, such as road

centrelines and road markings. To avoid the loss of essential information when interpolating mobile LiDAR data, seamless integration of the third-party software packages is urgently needed. Furthermore, a common data exchange platform should be considered for transportation agencies to improve data interoperability.

5. Conclusions

Roads play a vital role in people's daily lives in all countries because it brings people together for business or pleasure by connecting small and large cities, urban and rural communities, as well as connecting a country with its neighbours to enable the safe movement of goods, people and services. To safely keep people on the move, transportation departments in cities or countries have to periodically perform road surveys. The documentation of road features includes both road surface geometry (e.g. lane width, number of lanes, longitudinal slopes and transverse slopes) and road environment (e.g. road markings, pavement cracks, street signs, trees, vegetation and traffic light poles). The surveyed data are used not only for transportation departments to maintain, rehabilitate and reconstruct the current roadways and bridges, and to manage traffic and parking infrastructure, but also for administration to assess policies and practices affecting roadways. A mobile LiDAR system, mounted on the top of a vehicle, captures virtually anything visible to the eyes in the form of 3D point clouds with real-world coordinates, thereby providing accurate 3D geospatial information of roadways. To date, the feasibility of mobile LiDAR technology for road surveys has been proven for safety, cost, efficiency and data confidence. Given these mobile LiDAR systems' advantages, as mentioned in most reports, research articles, presentations at conferences or short web articles, a growing number of transportation agencies have been considering mobile LiDAR for road information inventory.

In this work, a review of the ability of mobile LiDAR systems to road information inventory was described. This review includes a discussion of system configuration, direct geo-referencing and the analysis of data quality, and current road-scene applications. The main distinction produced by the review identifies that the systems are ideal for road information inventory and transportation-related applications.

Mobile LiDAR systems are gaining widespread acceptance with time. With the continuous advancement of mobile LiDAR technology, as well as the reduced costs of system development, it can be expected that both mobile LiDAR technologies and data processing techniques will be further explored in road information inventory. The literature review reveals that studies on mobile LiDAR technology as a reliable and cost-effective alternative is worthwhile for carrying out road inspections along the route corridor.

Disclosure statement

No potential conflict of interest was reported by the authors.

Funding

This work was supported by the National Natural Science Foundation of China [grant number 41501501]; Natural Science Foundation of Jiangsu Province [grant number BK20151524].

References

Abuhadrous, A., *et al*., 2004. Digitizing and 3D modeling of urban environments and roads using vehicle borne laser scanner system. *In*: *2004 IEEE/RSJ international conference on intelligent robots and systems*, 28 September–2 October 2004, Sendai. IEEE, 76–81.

Aijazi, A., Checchin, P., and Trassoudaine, L., 2013. Segmentation based classification of 3d urban point clouds: a super-voxel based approach with evaluation. *Remote Sensing*, 5, 1624–1650. doi:10.3390/rs5041624

Barber, D., Mills, J., and Smith-Voysey, S., 2008. Geometric validation of a ground-based mobile laser scanning system. *ISPRS Journal of Photogrammetry and Remote Sensing*, 63, 128–141. doi:10.1016/j.isprsjprs.2007.07.005.

Beraldin, J., Blais, F., and Lohr, U., 2010. Laser scanning technology. *In*: G. Vosselman and H. Mass, eds. *Airborne and terrestrial laser scanning*. Caithness: Whittles Publishing, 1–42.

Bertozzi, M., *et al*., 1997. Obstacle and lane detection on the ARGO autonomous vehicle. *In*: *Proceedings of IEEE intelligent transportation systems conference*, 10–13 November, Boston, MA. IEEE, 1010–1015.

Boyko, A. and Funkhouser, T., 2011. Extracting roads from dense point clouds in large scale urban environment. *ISPRS Journal of Photogrammetry Remote Sensing*, 66, S2–S12. doi:10.1016/j.isprsjprs.2011.09.009

Brenner, 2009a. Global localization of vehicles using local pole patterns. *In*: *Proceedings of the DAGM 2009, 31st annual symposium of the German association for pattern recognition, Springer LNCS 5748*. Berlin: Springer, 61–70.

Brenner, 2009b. Extraction of features from mobile laser scanning data for future driver assistance systems. *In*: M. Sester, *et al*., eds. *Advances in GIScience*. Lecture Notes in Geoinformation and Cartography. Berlin: Springer, 25–42.

Bruton, A.M., 2000. *Improving the accuracy and resolution of SINS/DGPS airborne gravimetry*. Thesis (PhD). University of Calgary, UCGE Report #20145.

Cabo, C., García Cortés, S., and Ordoñez, C., 2015. Mobile Laser Scanner data for automatic surface detection based on line arrangement. *Automation in Construction*, 58 (2015), 28–37. doi:10.1016/j.autcon.2015.07.005

Cabo, C., *et al*., 2014. An algorithm for automatic detection of pole-like street furniture objects from mobile laser scanning point clouds. *ISPRS Journals of Photogrammetry and Remote Sensing*, 87, 47–56. doi:10.1016/j.isprsjprs.2013.10.008

Carnaby, B., 2005. Poor road markings contribute to crash rates. *In*: *Australasian road safety research policing education conference*, 14–16 November 2005 Wellington, CD-ROM (CD401).

Chen, X., Stroila, M., and Wang, R., 2009. Next generation map marking: geo-referenced ground-level LiDAR point clouds for automatic retro-reflective road feature extraction. *In*: *17th ACM SIGSPATIAL international conference on advances in geographic information system*, 4–6 November 2009 Seattle, WA, (on CD-ROM).

Chen, Y., Zhao, H., and Shibasaki, R., 2007. A mobile system combining laser scanners and cameras for urban spatial objects extraction. *In*: *Proceedings of IEEE conference on machine learning and cybernetics*, 19–22 August, Hong Kong, 3. IEEE, 1729–1733.

Díaz-Vilariño, L., *et al*., 2016. Automatic classification of urban pavements using mobile LiDAR data and roughness descriptors. *Construction and Building Materials*, 102 (2016), 208–215. doi:10.1016/j.conbuildmat.2015.10.199

Dickmanns, E. and Mysliwetz, B., 1992. Recursive 3-D road and relative ego-state recognition. *IEEE Transactions on Pattern Analysis and Machine Intelligence*, 14 (2), 199–213. doi:10.1109/34.121789

Duffell, C.G. and Rudrum, D.M., 2005. Remote sensing techniques for highway earthworks assessment. *In*: *Proceedings of GeoFrontiers 2005*, 24–26 January, Austin, TX. American Society of Civil Engineers (ASCE), 1–13.

DYNASCAN MDL, 2016. *Homepage of the company MDL laser systems* [online]. Available from: http://www.mdl.co.uk [Accessed 4 January 2016].

El-Halawany, S.I. and Lichti, D.D., 2011. Detection of road poles from mobile terrestrial laser scanner point cloud. *In*: *Proceedings of international workshop multi-platform/multi-sensor remote sensing mapping*, 10–12 January, Xiamen. IEEE, 1–6.

El-Halawany, S.I. and Lichti, D.D., 2013. Detecting road poles from mobile terrestrial laser scanning data. *Geosciences & Remote Sensing*, 50 (6), 704–722.

Fan, H., Yao, W., and Tang, L., 2014. Identifying man-made objects along urban road corridors from mobile lidar data. *IEEE Geoscience and Remote Sensing Letters*, 11 (5), 950–954. doi:10.1109/LGRS.2013.2283090

Faro, 2016. *Homepage of the company FARO laser scanner focus^{3D}* [online]. Available from: http://www.faroasia.com/home/CN/ [Accessed 4 January 2016].

Glennie, C., 2007. Rigorous 3D error analysis of kinematic scanning LIDAR systems. *Journal of Applied Geodesy*, 1 (2007), 147–157. doi:10.1515/jag.2007.017

Glennie, C., 2009. Kinematic terrestrial light-detection and ranging system for scanning. *Transportation Research Record*, 2105, 135–141. doi:10.3141/2105-17

Glennie, C., *et al*., 2013. Compact multipurpose mobile laser scanning system-initial tests and results. *Remote Sensing*, 5, 521–538. doi:10.3390/rs5020521

Golovinskiy, V.K. and Funkhouser, T., 2009. Shape-based recognition of 3d point clouds in urban environments. *In*: *Proceedings of IEEE 12th international conference on computer vision*, 27 September–4 October, Kyoto. IEEE, 2154–2161.

Gordon, P., 2010. 3D scanning: high-definition mobile mapping. *Professional Surveyor Magazine*. [Accessed 4 March 2016].

Goulette, F., *et al*., 2008. An integrated on-board laser range sensing system for on-the-way city and road modelling [Unformatted CD-ROM]. *In*: *International archives of the photogrammetry, remote sensing and spatial information sciences, ISPRS*, 34 (Part XXX). Göttingen: Copernicus Publications.

Guan, H., Li, J., and Yu, Y., 2013. 3D urban mapping using a Trimble MX8 mobile laser scanning system: a validation study. *In*: *MMT 2013*, 1–3 May 2013 Taiwan

Guan, H., *et al*., 2014a. Using mobile laser scanning data for automated extraction of road markings. *ISPRS Journal of Photogrammetry & Remote Sensing*, 87, 93–107. doi:10.1016/j.isprsjprs.2013.11.005

Guan, H., *et al*., 2014b. Automated extraction of manhole covers using mobile LiDAR data. *Remote Sensing Letters*, 5 (12), 1042–1050. doi:10.1080/2150704X.2014.994716

Guan, H., *et al*., 2015a. Iterative tensor voting method for crack detection using mobile laser scanning data. *IEEE Transactions on Geoscience & Remote Sensing*, 53 (3), 1527–1537. doi:10.1109/TGRS.2014.2344714

Guan, H., *et al*., 2015b. Using mobile LiDAR data for rapidly updating road markings. *IEEE Transactions on Intelligence Transportation Systems*, 16 (5), 2457–2465. doi:10.1109/TITS.2015.2409192

Guo, J., Tsai, M., and Han, J., 2015. Automatic reconstruction of road surface features by using terrestrial mobile lidar. *Automation in Construction*, 58 (2015), 165–175. doi:10.1016/j.autcon.2015.07.017

Haala, N., *et al*., 2008. Mobile lidar mapping for urban data capture. *In*: M. Loannides, *et al*., eds. *14th international conference on virtual systems and multimedia*, 20–26 October, Limassol. Virtual Systems and Multimedia Society, 95–100.

Hata, A.Y., Osorio, F.S., and Wolf, D.F., 2014. Robust curb detection and vehicle localization in urban environments. *In*: *2014 IEEE intelligent vehicles symposium (IV)*, 8–11 June 2014 Dearborn, MI.

Hernandez, J. and Marcotegui, B., 2009. Filtering artifacts and pavement segmentation from mobile LiDAR data. *In*: Bretar, *et al*., eds. *Laserscanning – IAPRS 2009*, 1–2 September, Paris. ISPRS, XXXVIII (Part3/W8), 329–333.

Hofmann, S. and Brenner, C., 2009. Quality assessment of automatically generated feature maps for future driver assistance systems. *In*: *Proceedings of the 17th ACM SIGSPATIAL international conference on advances in geographic information systems*, 4–6 November 2009 Seattle, WA. ACM, 500–503.

Hu, Y., *et al*., 2011. A novel approach to extracting street lamps from vehicle-borne laser data. *In*: *Proceedings of IEEE conference on geoinformatics*, 24–26 June, Shanghai. IEEE, 1–6.

Iavarone, A., 2007. Feature: terrestrial LiDAR goes mobile. *Professional Surveyor Magazine*. [Accessed 4 January 2016].

Ibrahim, S. and Lichti, D., 2012. Curb-based street floor extraction from mobile terrestrial LiDAR point cloud. *ISPRS Archives*, 39 (Part B5), 193–198.

Jaakkola, A., *et al*., 2008. Retrieval algorithms for road surface modelling using laser-based mobile mapping. *Sensors*, 8, 5238–5249. doi:10.3390/s8095238

Jaakkola, A., *et al*., 2010. A low-cost multi-sensoral mobile mapping system and its feasibility for tree measurements. *ISPRS Journal of Photogrammetry and Remote Sensing*, 65, 514–522. doi:10.1016/j.isprsjprs.2010.08.002

Jacobs, G., 2005. Uses in transportation in high-definition surveying: 3D laser scanning. *Professional Surveyor Magazine*, vol. April.

Ji, S., Shi, Y., and Shi, Z., 2012. Manhole cover detection using vehicle-based multi-sensor data. *ISPRS Archives*, 25 August–1 September 2012 Melbourne, Australia, 39 (B3), 281–284.

Kukko, A., *et al*., 2009. Mobile mapping system and computing methods for modeling of road environment. *In*: *Proceedings of urban remote sensing event*, 20–22 May, Shanghai. IEEE, 1–6.

Kumar, P., *et al*., 2013. An automated algorithm for extracting road edges from terrestrial mobile LiDAR data. *ISPRS Journal of Photogrammetry and Remote Sensing*, 85 (2013), 44–55. doi:10.1016/j.isprsjprs.2013.08.003

Landa, J. and Prochazka, D., 2014. Automatic road inventory using LiDAR. *Procedia Economics and Finance*, 12, 363–370. doi:10.1016/S2212-5671(14)00356-6

Lehtomäki, M., *et al*., 2010. Detection of vertical pole-like objects in a road environment using vehicle-based laser scanning data. *Remote Sensing*, 2, 641–664. doi:10.3390/rs2030641

Leica, 2016. *Homepage of the company* [online]. Available from: http://hds.leica-geosystems.com/en/HDS-Laser-Scanners-SW_5570.htm [Accessed 4 January 2016].

Lemmens, M., 2011. Geo-information: technology, applications and the environment. *Geotechnologies and the Environment Series*, 5, 101–121.

Lichti, D., 2010. Terrestrial laser scanner self-calibration: correlation sources and their mitigation. *ISPRS Journal of Photogrammetric and Remote Sensing*, 65, 93–102. doi:10.1016/j.isprsjprs.2009.09.002

Lim, S., *et al*., 2013. Accuracy assessment of a mobile terrestrial lidar survey at Padre Island National Seashore. *International Journal of Remote Sensing*, 34 (18), 6355–6366. doi:10.1080/01431161.2013.800658

Lin, Y. and Hyyppä, J., 2010. Geometry and intensity based culvert detection in mobile laser scanning point clouds. *Journal of Applied Remote Sensing*, 4, 043553. doi:10.1117/1.3518442

Liu, Z., Wang, J., and Liu, D., 2013. A new curb detection method for unmanned ground vehicles using 2d sequential laser data. *Sensors*, 13, 1102–1120. doi:10.3390/s130101102

Manandhar, D. and Shibasaki, R., 2002. Auto-extraction of urban features from vehicle-borne laser data. *ISPRS Archives*, 34 (Part 4), 650–655.

Manandhar, D. and Shibasaki, R., 2001. Feature extraction from range data. *In*: *Proceedings of the 22nd Asian conference on remote sensing*, 5–9 November 2001, Singapore.

Mancini, A., Frontoni, E., and Zingaretti, P., 2012. Automatic road object extraction from mobile mapping systems. *In*: *Conference: Proceedings of 2012 8th IEEE/ASME International Conference on Mechatronic and Embedded Systems and Applications*, 8–10 July 2012 Suzhou.

McElhinney, C.P., *et al*., 2010. Initial results from European road safety inspection (EURSI) mobile mapping project. *ISPRS Archives*, 38 (Part 5), 440–445.

Munoz, D., Vandapel, N., and Hebert, M., 2008. Directional associative Markov network for 3-d point cloud classification. *In*: *4th international symposium on 3D data processing, visualization and transmission*, 18–20 June 2008 Atlanta, GA.

Olsen, M.J., *et al*., 2013. *Guidelines for the use of mobile LIDAR in transportation applications*. Washington, DC: TRB, p. 250 (TRB NCHRP Final Report 748).

Optech Lynx, 2016. *Homepage of the company Optech*. Available from: http://www.teledyneoptech.com/index.php/products/mobile-survey/ [Accessed 4 January 2016].

Petrie, G. and Toth, C., 2008. Introduction to laser ranging, profiling, and scanning. *In*: J. Shan and C.K. Toth, eds. *Topographic laser ranging and scanning: principles and processing*. Boca Raton, FL: CRC Press, Taylor & Francis Group, 1–27.

Pikus, I.M., 2006. *Manhole security: protecting America's critical underground infrastructure*. White Paper, 2006. Washington, DC: National Strategies, Inc.

Pomerleau, D. and Jochem, T., 1996. Rapidly adapting machine vision for automated vehicle steering. *IEEE Expert*, 11, 19–27. doi:10.1109/64.491277.

Pu, S., *et al*., 2011. Recognizing basic structures from mobile laser scanning data for road inventory studies. *ISPRS Journal of Photogrammetry and Remote Sensing*, 66 (6), S28–S39. doi:10.1016/j.isprsjprs.2011.08.006

Puente, I., *et al*., 2013a. Review of mobile mapping and surveying technologies. *Measurement*, 46, 2127–2145. doi:10.1016/j.measurement.2013.03.006

Puente, I., *et al*., 2013b. Accuracy verification of the Lynx Mobile Mapper system. *Optics & Laser Technology*, 45, 578–586. doi:10.1016/j.optlastec.2012.05.029

Puente, I., *et al*., 2014. Automatic detection of road tunnel luminaires using a mobile LiDAR system. *Measurement*, 47 (1), 569–575. doi:10.1016/j.measurement.2013.09.044

Puttonen, I., *et al*., 2013. Improved sampling for terrestrial and Mobile Laser Scanner point cloud data. *Remote Sensing*, 5 (4), 1754–1773. doi:10.3390/rs5041754

Rieger, P., *et al*., 2010. Boresight alignment method for mobile laser scanning systems. *Journal of Applied Geodesy*, 4 (1), 13–21. doi:10.1515/jag.2010.002

RIEGL, 2016. *Homepage of the company RIEGL laser measurement systems GmbH*. Available from: http://www.riegl.com/ [Accessed 4 January 2016].

Riveiro, B., *et al*., 2016. Automatic segmentation and shape-based classification of retro-reflective traffic signs from mobile lidar data. *IEEE Journal of Selected Topics in Applied Earth Observations and Remote Sensing*. doi:10.1109/JSTARS.2015.2461680.

Riveiro, B., *et al*., 2015. Automatic detection of zebra crossings from mobile LiDAR data. *Optical & Laser Technology*, 70 (2015), 63–70. doi:10.1016/j.optlastec.2015.01.011

Rybka, R., 2011. Autodesk and Bentley systems talk about mobile LiDAR. *LiDAR*, 1 (2), 41–44.

Shen, Y., *et al*., 2008. Feature extraction from vehicle-borne laser scanning data [Unformatted CD-ROM]. *In*: *International conference on earth observation data processing and analysis (ICEODPA)*, 30 December 2008 Wuhan. SPIE, 7285.

Sick, 2016. *Homepage of the Company SICK laser scanners*. Available from: http://www.sick.com/group/EN/home/products/product_portfolio/optoelectronic_protective_devices/Pages/safetylaserscanners_s3000.aspx [Accessed 4 January 2016].

Smadja, L., Ninot, J., and Gavrilovic, T., 2010. Road extraction and environment interpretation from Lidar sensors. *ISPRS Achieves*, 38, 281–286.

Stauth, D. and Olsen, M., 2013. *Mobile LiDAR technology expanding rapidly* [online]. Available from: http://oregonstate.edu/ua/ncs/archives/2013/mar/mobile-lidar-technology-expanding-rapidly [Accessed 4 January 2016].

Takashi, O. and Kiyokazu, T., 2006. Lane recognition using on-vehicle LIDAR. *In*: *IEEE intelligent vehicle symposium*, 13–15 June, Tokyo. IEEE, 540–545.

Teo, T. and Chiu, C., 2016. Pole-Like road object detection from mobile lidar system using a coarse-to-fine approach. *IEEE Journal of Selected Topics in Applied Earth Observations and Remote Sensing*, doi:10.1109/JSTARS.2015.2467160.

Toth, C., 2009. R&D of mobile lidar mapping and future trends [Unformatted CD-ROM]. *In*: *ASPRS annual conference*, 9–13 March, Baltimore, MD. ASPRS.

Toth, C., Paska, E., and Brzezinska, D., 2008. Using road pavement markings as good control for lidar data. *ISPRS Archives*, 37 (B1), 189–196.

Trimble, 2016. *Homepage of the company trimble 3D laser scanning*. Available from: http://www.trimble.com/3d-laser-scanning/index.aspx [Accessed 4 January 2016].

Tsogas, M., *et al*., 2011. Combined lane and road attributes extraction by fusing data from digital map, laser scanner and camera. *Information Fusion*, 12, 28–36. doi:10.1016/j.inffus.2010.01.005

Velodyne, 2016. *Homepage of the Company Velodyne LiDAR systems*. Available from: http://velodynelidar.com/ [Accessed 4 January 2016].

Vosselman, G., 2009. Advanced point cloud processing. *In*: *Photogrammetric Week'09*, 3 July, Heidelberg. ISPRS, 137–146.

Wang, H., *et al*., 2012. Automatic road extraction from mobile laser scanning data. *In*: *International conference on computer vision in remote sensing (CVRS)*, 16–18 December 2012 Xiamen, China.

Williams, K., *et al*., 2013. Synthesis of transportation applications of mobile LiDAR. *Remote Sensing*, 5, 4652–4692. doi:10.3390/rs5094652

Yan, W., *et al*., 2016. Automatic extraction of highway light poles and towers from mobile LiDAR data. *Optics & Laser Technology*, 77, 162–168.

Yang, B. and Dong, Z., 2013. A shape-based segmentation method for mobile laser scanning point clouds. *ISPRS Journal of Photogrammetry and Remote Sensing*, 81, 19–30. doi:10.1016/j.isprsjprs.2013.04.002

Yang, B., Fang, L., and Li, J., 2013. Semi-automated extraction and delineation of 3D roads of street scene from mobile laser scanning point clouds. *ISPRS Journal of Photogrammetry and Remote Sensing*, 79 (2013), 80–93. doi:10.1016/j.isprsjprs.2013.01.016

Yang, B., *et al*., 2012a. Automated extraction of road markings from mobile lidar point clouds. *Photogrammetric Engineering & Remote Sensing*, 78 (4), 331–338. doi:10.14358/PERS.78.4.331

Yang, B., *et al*., 2012b. Automated extraction of street-scene objects from mobile lidar point clouds. *International Journal of Remote Sensing*, 33 (18), 5839–5861. doi:10.1080/01431161.2012.674229

Yen, K.S., Ravani, B., and Lasky, T.A., 2011. *LiDAR for data efficiency, Washington State Department of Transportation* [online]. Available from: http://www.wsdot.wa.gov/research/reports/fullreports/778.1.pdf [Accessed 4 January 2016].

Yokoyama, H., *et al*., 2011. Pole-like objects recognition from mobile laser scanning data using smoothing and principal component analysis. *ISPRS Archives*, 38 (Part 5/W12), 115–120.

Yokoyama, H., *et al*., 2013. Detection and classification of pole-like objects from mobile laser scanning data of urban environments. *International Journal of CAD/CAM*, 13 (2), 31–40.

Yoon, J. and Crane, C.D., 2009. Evaluation of terrain using LADAR data in urban environment for autonomous vehicles and its application in the DARPA urban challenge. *In*: *Proceedings of ICROS-SICE international joint conference*, 18–21 August, Fukuoka. SICE, 641–646.

Yu, S., *et al*., 2007. 3D reconstruction of road surfaces using an integrated multi-sensory approach. *Optics and Lasers in Engineering*, 45, 808–818. doi:10.1016/j.optlaseng.2006.12.007

Yu, Y., *et al*., 2014a. Automated detection of road manhole and sewer well covers from mobile lidar point clouds. *IEEE Geoscience and Remote Sensing Letters*, 11 (9), 1549–1553. doi:10.1109/LGRS.2014.2301195

Yu, Y., *et al*., 2014b. Pairwise three-dimensional shape context for partial object matching and retrieval on mobile laser scanning data. *IEEE Geoscience and Remote Sensing Letters*, 11 (5), 1019–1023. doi:10.1109/LGRS.2013.2285237

Yu, Y., *et al*., 2015a. Learning hierarchical features for automated extraction of road markings from 3d mobile lidar point clouds. *IEEE Journal of Selected Topics on Applied Earth Observations and Remote Sensing*, 8 (2), 709–726. doi:10.1109/JSTARS.2014.2347276

Yu, Y., *et al*., 2015b. Semiautomated extraction of street light poles from mobile LiDAR point-clouds. *IEEE Transactions on Geosciences & Remote Sensing*, 53 (3), 1374–1386. doi:10.1109/TGRS.2014.2338915

Yu, Y., Guan, H., and Ji, Z., 2015c. Automated detection of urban road manhole covers using mobile laser scanning data. *IEEE Transactions on Intelligence Transportation Systems*. doi:10.1109/TITS.2015.2413812.

Yuan, X., Zhao, C., and Zhang, H., 2010. Road detection and corner extraction using high definition Lidar. *Information Technology Journal*, 9, 1022–1030. doi:10.3923/itj.2010.1022.1030

Z+F, 2016. *Homepage of the Company Z+F laser scanner systems*. Available from: http://www.zf-laser.com/Home.91.0.html [Accessed 4 January 2016].

Zhao, H. and Shibasaki, R., 2002. Surface modelling of urban 3d objects from vehicle-borne laser range data. *ISPRS Archives*, 34 (3/ A), 412–417.